Modeling Charged-Particle Spectra to Diagnose Asymmetries in OMEGA Implosions

Matthew Cufari

Pittsford Sutherland High School

Pittsford, NY

Advisors: Radha Bahukutumbi and Owen Mannion

Laboratory For Laser Energetics

University of Rochester

Rochester, NY

January 2019

Abstract:

Charged-particle spectra are used to diagnose implosion asymmetries in inertial confinement fusion (ICF) experiments on OMEGA. These asymmetries can be the result of numerous imperfections including beam mispointing, beam mistiming, and target offset and manifest as variations in the areal density of the target. These asymmetries cause reduced implosion performance and result in a less efficient conversion of laser energy to hot spot energy. For room-temperature D_2 experiments, the areal density can be inferred from the average energy of detected secondary protons. Asymmetries can then be inferred by comparing areal density measurements along multiple lines of sight. In cryogenic DT experiments, the areal density can be inferred from the knock-on deuteron energy spectrum. The Monte-Carlo code IRIS3D has been extended to simulate charged particles including secondary protons from D_2 targets and knock-on deuterons from DT targets. This was accomplished by integrating a stopping-power physics package into IRIS3D. IRIS3D generates energy spectra for secondary protons and knock-on deuterons by transporting charged particles in straight-line trajectories out of the ICF target to a synthetic detector. For room temperature implosions, IRIS3D computes the average energy of secondary protons along multiple lines of sight to infer areal density asymmetries around the target. In order to diagnose areal density asymmetries in cryogenic targets, an algorithm was developed to infer areal density based on the knock-on deuteron spectrum generated by IRIS3D. By post-processing hydrodynamic simulations with IRIS3D, direct comparisons can now be made with experimental data to infer areal density asymmetries.

1. Introduction:

Charged particle spectra are used to infer the extent of nonuniformity growth in OMEGA targets [1,2,3]. Room-temperature targets can be filled with D_2 gas surrounded by a plastic ablator. These targets are typically positioned within 5 μm of the desired position [4]. Positioning targets consistently within 5 μm of the desired position allows for very controlled experiments. In order to create a plasma, the target is irradiated by the OMEGA laser which heats the target and causes the plastic shell to ablate off, compressing the gas. As the target is compressed it heats the deuterium fuel to temperatures that enable the ions to fuse. D_2 fusion yields neutrons and ^{3}He nuclei. Some of the ^{3}He nuclei then collide with the background deuterium and fuse to form alpha particles and protons. The formed protons are referred to as secondary protons because they are the product of fusion from a primary D_2 fusion product. These protons escape the plasma and can be detected using various charged particle detectors such as wedge-range filters or charged-particle spectrometers. As these protons escape the plasma, they undergo a phenomenon called stopping-power whereby they are slowed down and lose some of their kinetic energy to the surrounding plasma [5]. Areal density is the dominant factor for determining the extent of the energy loss the secondary protons experience. Areal density is defined as

$$\rho R = \int_0^R \rho dr \qquad (1)$$

where ρ is mass density and R is the radius of the target. Energy loss increases linearly with areal density to values of approximately 250 mg/cm^2 for secondary protons.

The Monte-Carlo code IRIS3D is used to post-process hydrodynamic simulations by simulating the reactions that take place during an OMEGA implosion [6]. This is accomplished by simulating a fraction of the actual fusion reactions and tracking the fusion products to a synthetic detector. Increasing the number of simulated particles allows for higher resolution results, but also increases computation time. In this work,

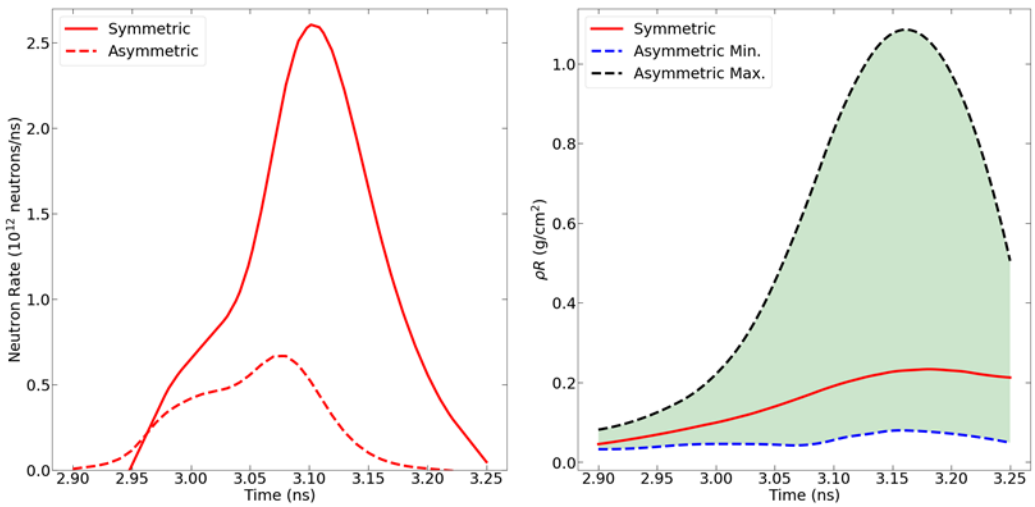

Figure 1: Neutron rate (left) and areal density (right) for a target at target chamber center (symmetric) and a target offset by 40 μm (asymmetric).

IRIS3D was extended to include a stopping-power physics package which computes the energy loss of charged particles over the simulation domain. As a charged particle is transported through the mesh to adjacent regions, the path the particle takes is broken into subsections over which the energy loss is computed. The particle may elastically collide with other fusion products in the mesh resulting in a change in direction and energy. This transport process is repeated until the particle enters a detector located outside of the target.

A set of room temperature D_2 targets were intentionally offset 40 μm from target chamber center to study the charged-particle spectra and target nonuniformity growth in large-offset shots. Post shot simulations have been processed through IRIS3D. Figure 1

compares the neutron rates and areal densities from IRIS3D simulations of a centered target and an offset target. In the offset shot the total neutron yield is reduced, and the time of peak neutron production occurs earlier as a result of the nonuniform compression of the target. The asymmetric target areal density min/max curves demonstrate that the areal density is different along different lines of sight. In the case of Figure 1, the maximum areal density curve is along the line of sight in the direction of the offset, and the minimum is along the line of sight opposite the direction of the offset. This curve demonstrates that charged particle energy spectra are dependent on the lines of sight. Nonuniformities can be inferred by comparing these spectra.

Cryogenic targets are filled with deuterium-tritium (DT) gas surrounded by a layer of DT ice. A plastic ablator encloses the target. In recent OMEGA cryogenic implosions, 86% of targets were positioned within 15 μm of the desired position [4]. Cryogenic targets implode and fuse, and the deuterium-tritium fuel forms neutrons and alpha particles as fusion products. The neutrons collide with and elastically scatter background deuterium and tritium ions [1,3]. Similar to secondary protons, these knock-on deuterons are slowed down as they travel through the plasma due to their non-zero electric charge. The knock-on deuteron energy spectra can then be used to diagnose nonuniformities in the target [1,3]. Scientists at MIT's Plasma Science and Fusion Center are currently working to use a comparison between detected knock-on deuteron spectra and simulated spectra to diagnose areal density asymmetries in OMEGA implosions.

2. Secondary Protons:

Room temperature implosions use gaseous fuel surrounded by a plastic shell. The targets are irradiated, and the plastic shell is ablated off driving the compression of

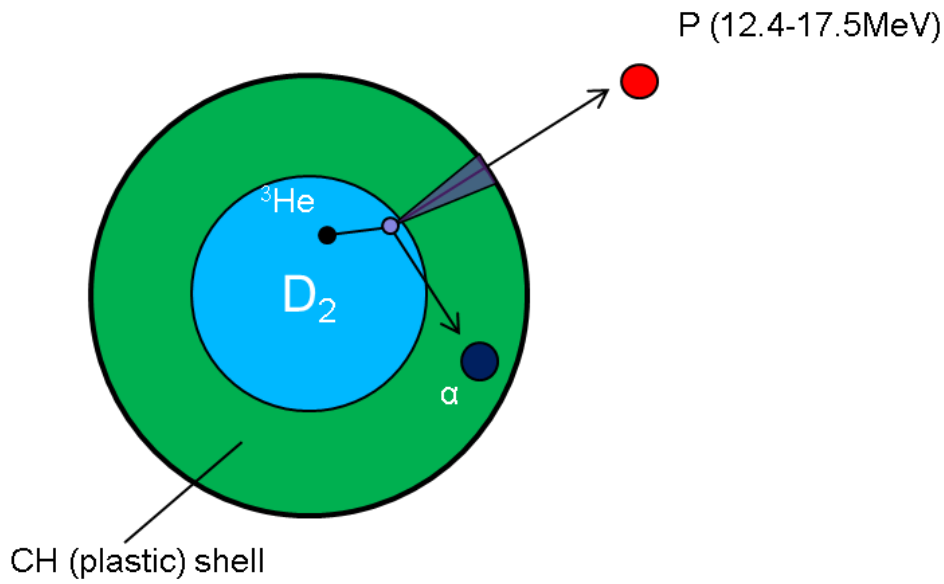

Figure 2: Cross section of a room temperature D_2 target. Both the ^{3}He and secondary proton undergo stopping power, losing energy to the surrounding plasma as they travel through the target.

the fuel. This compression produces conditions with sufficiently high temperatures and pressures that enable the fuel to undergo thermonuclear fusion. D_2 gas fuses according to the equation,

$$D + D \rightarrow {}^3He(0.82\ MeV) + n(2.45\ MeV) \qquad (2)$$

The resulting ^{3}He is capable of then fusing with background deuterium plasma forming an alpha particle and a proton (P) [2].

$${}^3He(< 0.82\ MeV) + D \rightarrow \alpha\ (1.7\text{-}6.6\ MeV) + P(12.4\text{-}17.5\ MeV) \qquad (3)$$

The ^{3}He product is produced at an initial energy of 0.82 MeV but loses energy quickly as a result of having a +2 nuclear charge. Due to its relatively low energy, ^{3}He does not travel a significant distance before stopping in the plasma. Figure 2 shows a ^{3}He

particle created in the D_2 fuel and undergoing a secondary reaction near the D_2/plastic interface. The secondary proton is slowed down while passing through the plastic shell.

IRIS3D uses spherically symmetric iceblock profiles as benchmarks before post-processing hydrodynamic simulations. The stopping-power algorithm was optimized and

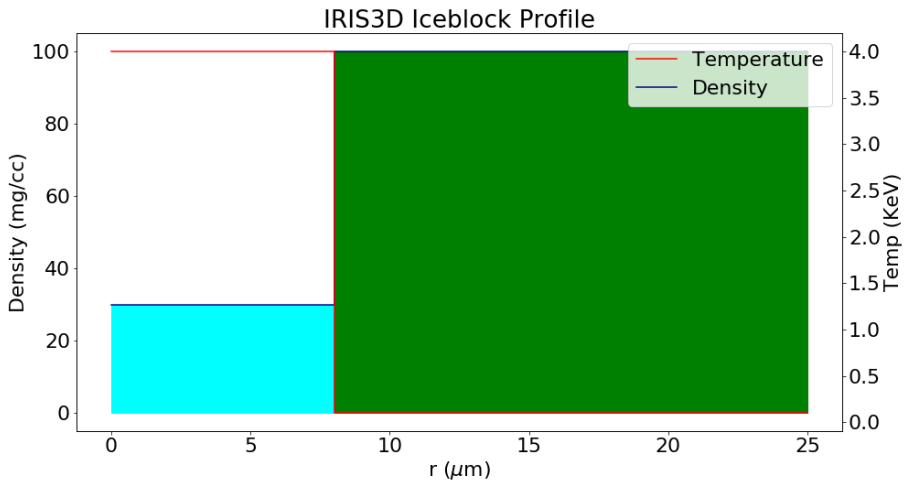

Figure 3: Simplified temperature and density plot for an imploded target. Cyan is D_2 gas. Green is the plastic shell. In the gaseous region of the profile, the density is low compared to the plastic region.

tested using iceblock models. An example of an iceblock profile is shown in Figure 3. The profile is characterized by temperature, density, and the ratio of elemental components. For example, the plastic may be composed of a 1:1 carbon to hydrogen ratio. In Figure 3, the iceblock model is characterized by a region of D_2 fuel of density 30 mg/cc that forms a sphere of radius 8 μm. Beyond the D_2 fuel, the iceblock model shows the plastic shell, which is much higher in density, 100 mg/cc, and lower in temperature, 0.1 keV. The plastic shell extends beyond 25 μm. More energy loss occurs in the shell due to the higher density compared to the fuel. Figure 3 is the first iceblock model in a series used to quantify a relationship between areal density and energy loss. Additional iceblocks have profiles with densities as large as 35 g/cc with radii which extend to 100 μm.

Areal density, defined in equation (1), is a useful quantity which can be used to infer target nonuniformity. In the absence of asymmetries, the plasma would have the same areal density at any viewing angle. Nonuniform compression, such as that which occurs when the target is offset, leads to areal density variations around the target. By comparing areal density measurements from different lines of sight, nonuniformities can be inferred.

Secondary protons are produced at locations near the hotspot of the plasma where ^{3}He fusion occurs. Secondary protons are emitted isotropically and will travel a path length which is different from the radius of the target. The secondary protons will experience an areal density given by,

$$\rho L = \int_0^L \rho dl \tag{4}$$

where L is the distance the proton travels from its birth location to the detector. In IRIS3D simulations, secondary protons are typically produced within 5 μm of the birth location of a ^{3}He. Spectra from these secondary protons are useful for inferring ρR_{fuel}, ρR_{Shell}, and ρR_{total} [2]. This is accomplished by comparing the measured proton energy and birth proton energy. Using this comparison, it is possible to compute the ρR of a target up to values where secondary protons are unable to escape the plasma.

The stopping power model used in IRIS3D is the Li-Petrasso stopping power model [5]. As a result of stopping power, particles in higher ρR targets will lose a greater

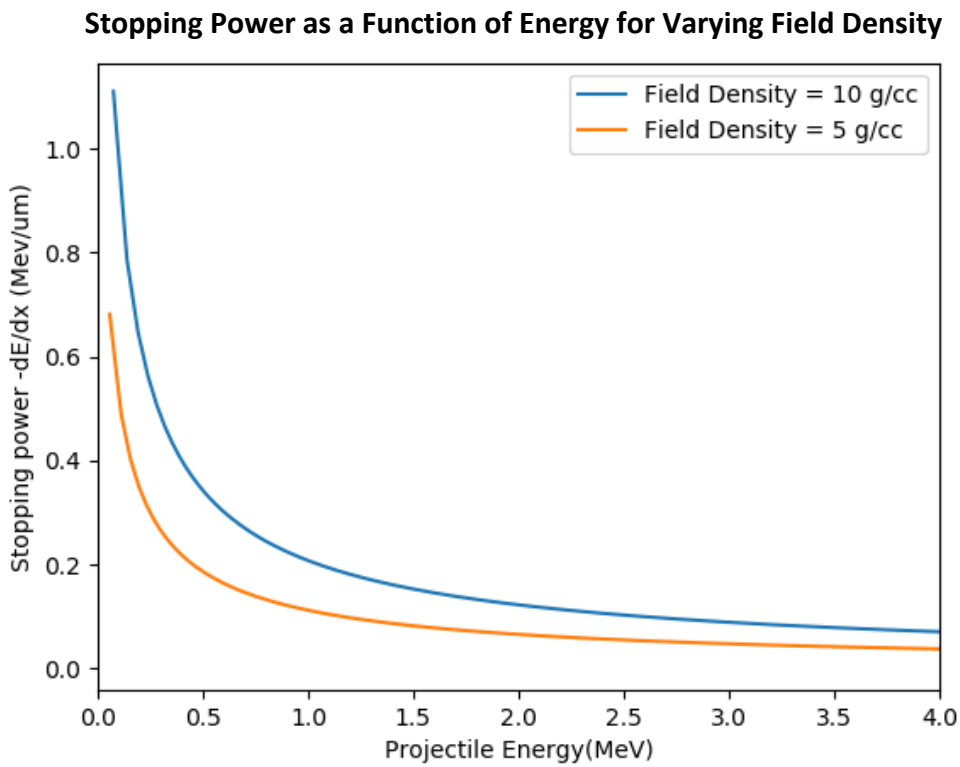

Figure 4: Plot showing energy loss for a proton with an initial energy of 4 MeV in differing field densities. The magnitude of stopping power is much larger for particles at low energies. As a result, particles born at low energies are less likely to be detected. Increased plasma density contributes to an overall increase in stopping power at all particle energies.

amount of energy compared with lower ρR targets. Figure 4 shows a plot of the magnitude of stopping power for a 4.0 MeV proton in two different plasma densities. Figure 4 demonstrates that the magnitude of the stopping power increases as particles lose energy to the surrounding field and that increased plasma density results in an increase in stopping power. Furthermore, charged particles in high areal density implosions may become trapped in the plasma. For example, secondary protons can escape areal densities below ~350 mg/cm^2. This makes secondary protons especially

useful as a diagnostic for ρR asymmetries in implosions with areal densities less than 350 mg/cm^2.

Stopping power is highly linear at high particle energies and low ρR values. By comparing the mean energy of secondary protons with varying areal density in iceblock

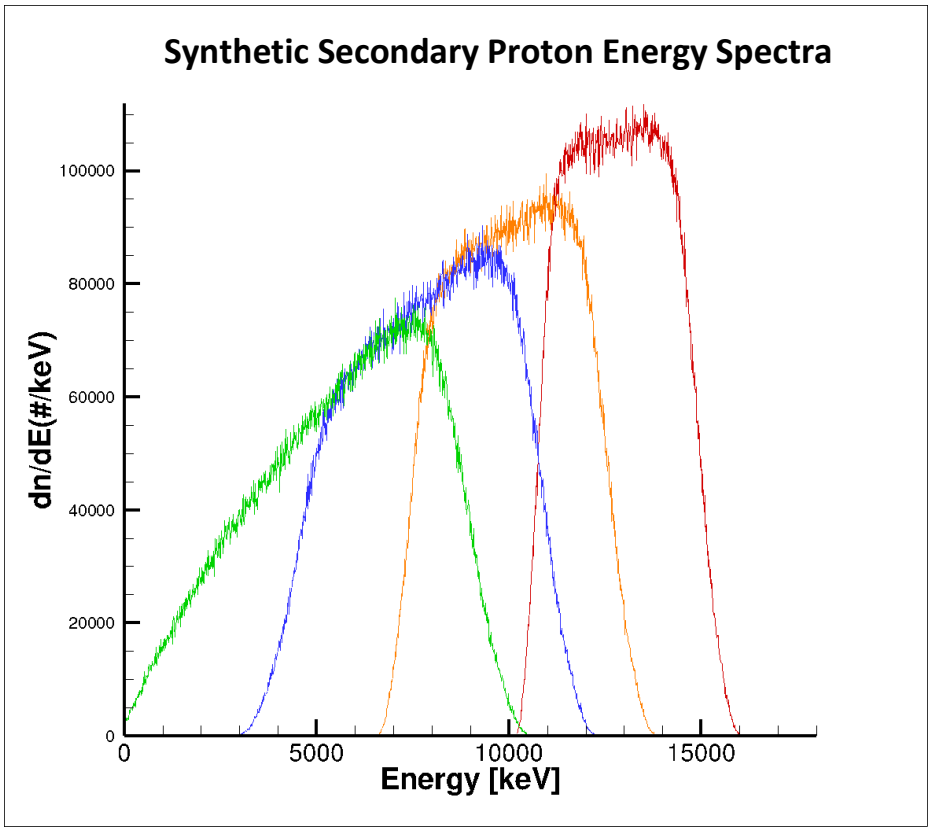

Figure 5: A plot showing secondary proton energy spectra for varying areal-density values. 50 mg/cm^2 (red), 100 mg/cm^2 (orange),150 mg/cm^2 (blue), 200 mg/cm^2 (green). Spectra were calculated from IRIS3D iceblock models of varying plasma density.

models, a one-to-one function was derived between areal density and average secondary proton energy. The correlation between average energy and areal density is apparent in Figure 5: secondary protons in a simulated implosion with areal density 50 mg/cm^2 have an average energy of ~12.5 MeV (red curve) whereas secondary protons in a simulated implosion with areal density 100 mg/cm^2 have an average energy

of ~10.3 MeV. As areal densities approach values of ~200 mg/cm^2, some secondary protons are unable to escape the plasma, resulting in a bias in the average energy. The average energy is only computed for those protons which have trajectories and initial energies that are sufficient to escape the plasma and be detected, resulting in a positively skewed calculation.

Figure 6 shows the mean energy of secondary protons in symmetric targets for increasing values of ρR. For low areal densities, the temperature of the plasma has little effect on the mean energy of the secondary protons. However, as areal densities increase, the resulting energy of the secondary protons becomes comparable to the

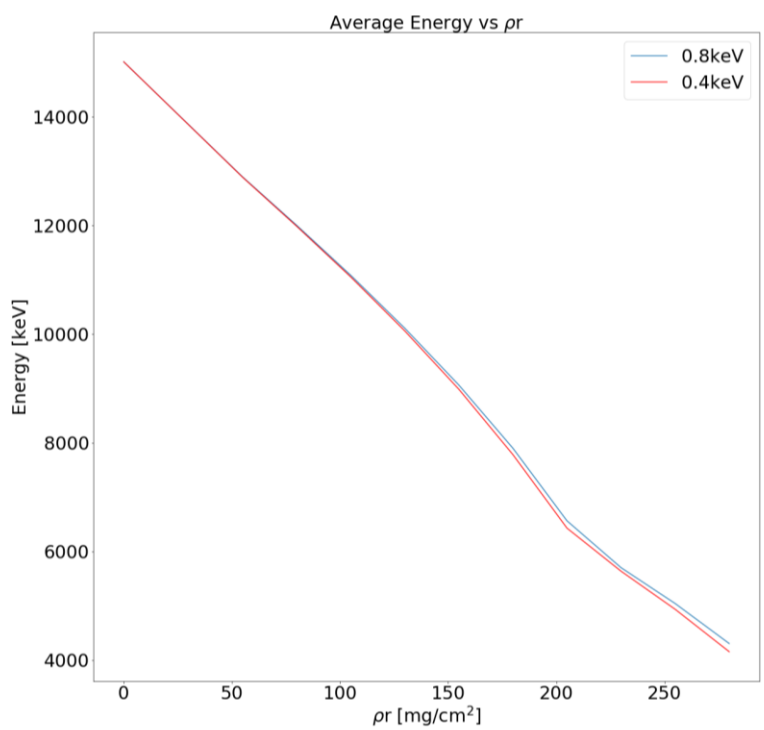

Figure 6: Plot of average energy of secondary protons vs areal density. The blue curve shows secondary protons in a plasma with a temperature of 0.8 keV and the red curve is for secondary protons in a plasma with a temperature of 0.4 keV

energy of the particles in the plasma. The change in functional form occurs abruptly at ~200 mg/cm^2 because some secondary protons produced at energies of ~12.4 MeV are unable to escape the target at this areal density. As a result of the increased stopping

power in lower temperatures, cooler plasmas have a lower ρR threshold at which the secondary proton diagnostic remains viable. At lower energies and cooler temperatures, stopping power becomes increasingly model dependent [7].

A linear fit to the graph in Figure 6 provides a relationship between mean energy and areal density of the form,

$$E(\rho R) = m * \rho R + Eo \quad (5)$$

where E(ρR) is the mean energy as a function of ρR, m is energy loss in keV/mg/cm^2, Eo is the mean energy in keV of a secondary proton at birth (14,950 keV). m has a value of ~ -41.186 keV/mg/cm^2. In order to infer the areal density of a target along a particular line of sight, the mean energy of the secondary protons is calculated from the detected spectra and the areal density is then computed using the inverse of the function above, which has the form,

$$\rho R(E) = \frac{E - Eo}{m} \quad (6)$$

where E is the average energy from the detector.

Figure 7 shows a hydrodynamic profile calculated by the code DRACO for an offset target at peak neutron production. DRACO is a two-dimensional hydrodynamic code which simulates the physics of the implosion. The hydrodynamic simulation is then post-processed by IRIS3D. IRIS3D generates synthetic spectra which can be compared with measured spectra from the implosion. In order to post-process DRACO simulations, which are two-dimensional, IRIS3D assumes rotational symmetry in phi. For shot 88581, target offset is the dominant source of nonuniformity. The target offset results in an *l=1* mode which is rotationally symmetric in phi [4]. The offset resulted in a

region of high density in the direction of the offset, which corresponds to a higher

DRACO Profile of Shot 88581 at Peak
Neutron Production

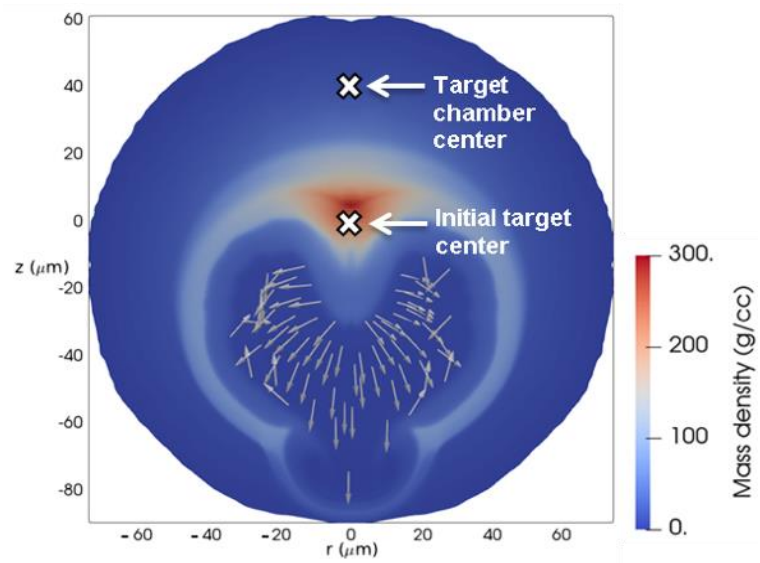

Figure 7: A 2-D DRACO profile for shot 88581, which had a 40 um offset along the line of sight of detector TIM 6. The shot was reoriented in IRIS3D such that the offset was 40 um in the direction of the north pole of the target. IRIS3D assumes symmetry in phi in order to post-process the 2D simulation

expected ρR value along a line of sight aimed at the north pole.

Figure 8 shows the inferred areal density values from post-shot simulations of shot 88581 and the positions of the wedge range filters (WRF) around the target. The inferred areal density values were computed using Eq. (6) by post-processing the DRACO simulation of shot 88581 to obtain the mean energy values. Based on this plot, WRF3, near the south pole of the target, should observe a spectrum that is significantly different than the spectrum seen observed by WRF2, which is near the north pole facing a high-density region. The secondary proton spectrum at WRF2 should be significantly downshifted and broadened compared to WRF3. The spectrum at WRF3 is expected to

yield a mean energy value of ~12.5 MeV. Future work will be done to compare the measured and simulated spectra.

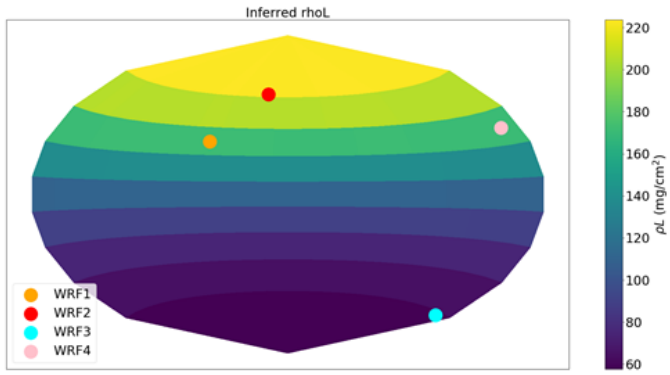

Figure 8: Hammer plot showing inferred ρL for shot 88581. The inferred areal density values were computed from equation (6)

3. Knock-on deuterons:

Knock-on deuterons are the product of an elastic collision between a neutron produced from DT fusion and a deuterium nucleus. Knock-on deuterons are produced in cryogenic targets and are useful for diagnosing areal-density asymmetries. Deuterium and tritium fuse according to,

$$D + T \rightarrow n\ (14.1\ \text{MeV}) + \alpha \qquad (7)$$

while under high pressure and temperature [1]. The neutron may then collide with background deuterium nuclei in an elastic collision,

$$D + n(14.1\text{MeV}) \rightarrow D'(\leq 12.5\ \text{MeV}) + n'. \qquad (8)$$

The resulting energy loss of D' as it exits the target makes the knock-on deuteron energy spectra useful for computing target areal densities. The unshifted deuteron energy spectrum is characterized by a peak formed between 12.5 MeV and 9.6 MeV. The spectrum trends upward from 9.6 to 0.0 MeV (the black curve in Figure 10 shows

the unshifted spectrum). Integrating under the peak of the unshifted knock-on deuteron spectrum yields an effective number of particles which contains ~15.7% of the knock-on yield [1,3].

As target ρR increases, the effective number of particles increases in proportion

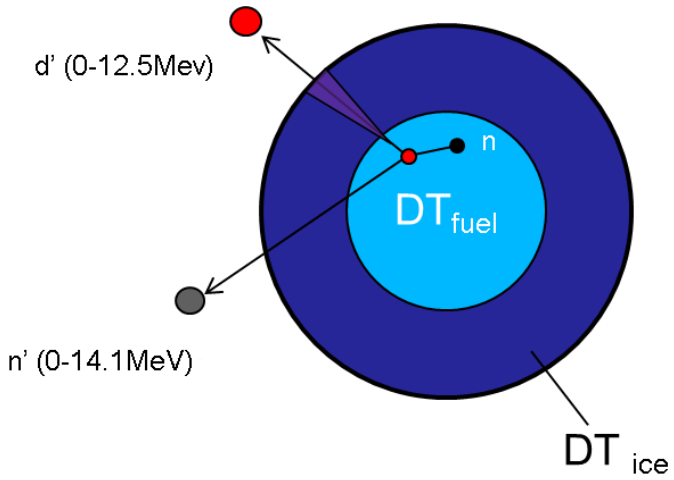

Figure 9: Schematic of production of a knock-on deuteron (denoted by d'). The knock-on-deuteron is formed from an elastic collision with a primary DT neutron. The deuteron experiences energy loss due to stopping power because of its positive charge.

to ρR [3]. However, as areal densities reach values >80 mg/cm^2, the characteristic peak is no longer identifiable as a result of the distortion of the knock-on deuteron spectrum from stopping power [1,3].

In a collision between a deuterium nucleus and a 14.1 MeV neutron, the deuterium nucleus scatters off with an energy between 0 MeV and 12.5 MeV. Figure 9 shows the knock-on deuteron losing energy to the background plasma due to stopping power, similar to the secondary proton. As the spectrum is downshifted, the ratio between the effective number of particles (the area beneath the peak) and total knock-on yield (area beneath the entire spectrum) grows in direct proportion to the ρR of the target [1,3].

Knock-on deuteron spectra are useful for diagnosing areal density asymmetries because the spectrum changes shape for small differences in ρR for areal densities greater than 80 mg/cm^2. At these higher areal densities, the peak of the unshifted knock-on deuteron spectrum (9.6 MeV-12.5 MeV), is washed out by the stopping power of the plasma. However, the spectrum is sensitive to small changes in areal densities and is therefore a useful tool for diagnosing target asymmetries. By comparing two spectra from different detectors with simulated spectra, one can infer the extent of nonuniformity.

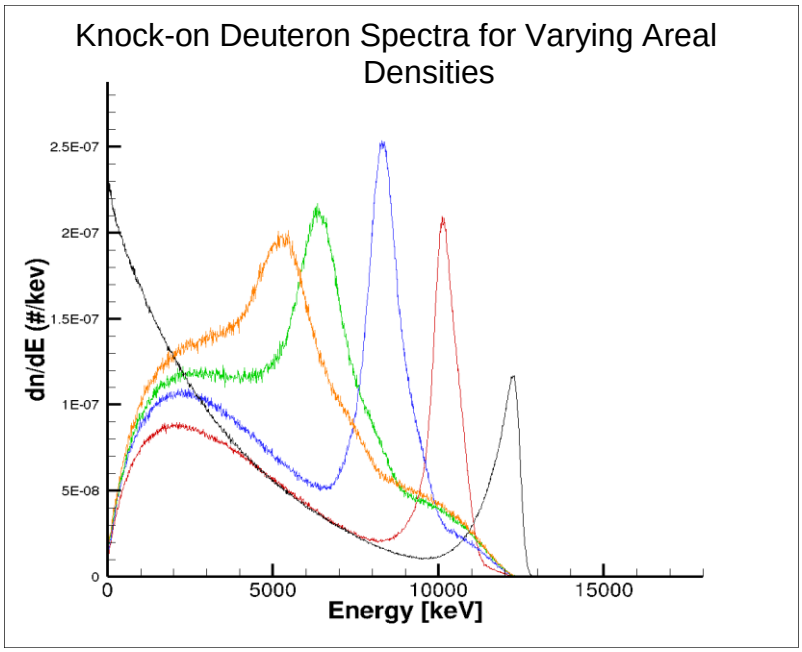

Figure 10: Knock-on deuteron spectra for varying areal density values. 0 mg/cm^2 (black), 15 mg/cm^2 (red), 30 mg/cm^2 (blue), 45 mg/cm^2 (green), 60 mg/cm^2 (orange). The peak becomes difficult to distinguish as areal density increases beyond 80 mg/cm^2. Spectra were produced using iceblock models.

Knock-on deuteron spectra, as shown in Figure 10, are characterized by a distinct peak in low-areal-density implosions. The peak becomes downshifted and broadened by stopping power as the areal density of the target increases. The total

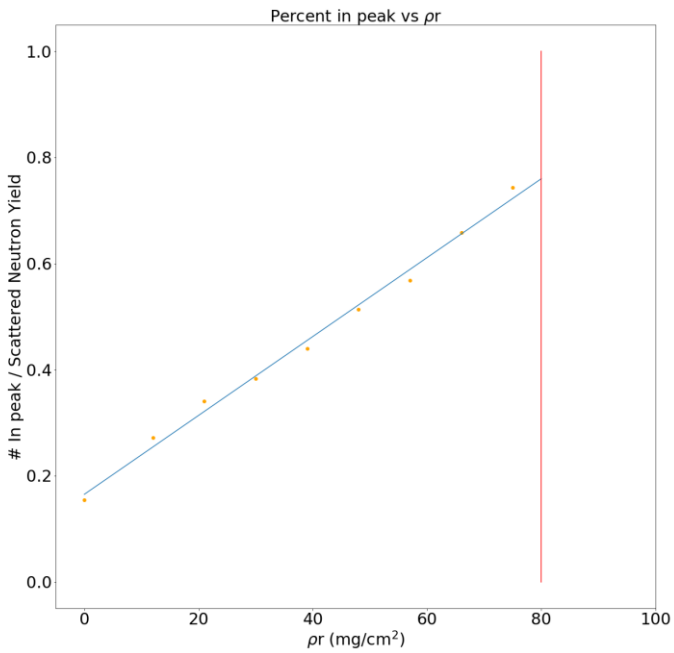

Figure 11: A scatter plot (orange points) showing the ratio between the knock-on deuteron yield within the peak and the total scattered neutron yield with a best fit line (blue) drawn. The red line corresponds to the areal density at which the peak is no longer distinguishable within the knock-on deuteron spectrum.

knock-on deuteron yield increases in proportion to areal density. The equation,

$$Y_{eff}/Y_{KOD} = k * \rho R + r_o \tag{9}$$

is then deduced where the ratio of the yield underneath the peak to the total yield is given by Y_{eff}/Y_{KOD} and r_o (=15.7%) is the ratio for a target with $\rho R = 0$ [1], Y_{eff} is defined as

$$Y_{eff} = \int_a^b N(E)dE \tag{10}$$

where N(E) represents the knock-on deuteron yield at energy E, and a and b are the bounds on the peak of the spectrum. To determine the areal density of targets with an areal density ≤80 mg/cm^2 the equation can be rearranged into the form,

$$\rho R = (Y_{eff}/Y_{KOD} - r_o) * k^{-1} \quad (11)$$

where k is a constant that corresponds to the change in the ratio between the effective yield and total yield with respect to a change in areal density.

In implosions where the areal density exceeds ~80 mg/cm^2, the knock-on deuteron spectrum is no longer characterized by a well-defined peak. Figure 11 illustrates that the ratio of the yield under the peak (Y_{eff}) to the total scattered neutron yield increases linearly with areal density until the peak of the knock-on deuteron spectrum is no longer distinguishable. Similar to the secondary proton spectrum, as areal density values increase, the number of knock-on deuterons unable to escape the plasma increases. It is possible to diagnose asymmetries by comparing the inferred areal density and shapes of the knock-on spectra from several detectors around a target.

4. Conclusion:

The Monte-Carlo particle tracking code IRIS3D was extended to model the behavior of charged particles in OMEGA implosions in order to develop two diagnostics for implosion asymmetries. Asymmetries in ICF implosions result in less efficient conversion of laser energy to hot spot energy, decreasing the total neutron yield.

One diagnostic applies to deuterium-deuterium fusion. Secondary protons formed from the fusing of a helium-3 with a background deuterium nucleus are slowed

down from their birth energy as they leave the target by a phenomenon called stopping power. The amount of energy secondary protons lose while travelling through the target is directly proportional to the areal density of the target at high energy and low areal density. Therefore, an areal density can be inferred by comparing the mean energy of secondary protons emitted from the target. Asymmetries can then be diagnosed by comparing multiple measurements of secondary proton mean energy along different lines of sight.

The second diagnostic applies to deuterium-tritium cryogenic targets. Knock-on deuterons are deuterium nuclei that collide elastically with a neutron formed from deuterium-tritium fusion. After colliding, the knock-on deuteron will travel through the target and lose energy as a result of stopping power. The unshifted knock-on deuteron energy spectrum is characterized by a sharp peak between 9.6 MeV and12.5 MeV which can be seen in Figure 10. The energy range of the peak becomes downshifted and broadened in proportion to areal density. The effective yield is computed by integrating the area under the peak. The ratio between the effective yield and total knock-on yield is directly proportional to areal density. By comparing the ratio at varying areal density values, a linear fit was produced which can be used to determine the ρR of a target. The linear fit is only a viable diagnostic for areal densities less than ~80 mg/cm^2 because at areal densities greater than this threshold, the effective yield is indistinguishable within the knock-on spectrum. However, the knock-on deuteron energy spectrum remains useful for areal densities greater than 80 mg/cm^2 because the spectrum changes noticeably for small changes in areal density. In order to diagnose asymmetries in high-areal-density targets, one must compare the shape of the knock-on

deuteron spectrum from detectors around the target with simulated data to determine if the areal densities vary significantly. Future work will compare the simulated knock-on and secondary proton data with experiment for the first time.

Acknowledgements:

I would like to thank my advisors, Dr. Radha Bahukutumbi and Owen Mannion, for their assistance on this project. Their insights and help were invaluable assets over the course of the summer. I would also like to thank Sam Miller for developing and testing the DRACO-IRIS3D converter, which allowed the DRACO simulations to be post-processed by IRIS3D. Also, Duc Cao verified IRIS3D calculations and helped to produce some of the figures in this paper and Yanhao Ding assisted in the integration of stopping power into IRIS3D.

I would also like to acknowledge my colleagues working in the high school research program for their insights and ability to facilitate a collaborative environment. Lastly, I would like to thank Dr. Craxton for running the high school research program and the opportunity to work at LLE.

References:

1. C.K. Li et al., *Study of direct-drive, deuterium–tritium gas-filled plastic capsule implosions using nuclear diagnostics at OMEGA,* Phys. Plasmas **8,** 4902 (2001)
2. F.H. Seguin, et al., *Using secondary-proton spectra to study the compression and symmetry of deuterium filled capsules at OMEGA.* Phys. Plasmas **9,** 2725 (2002)

3. P.B. Radha et al., *A novel charged-particle diagnostic for compression in inertial confinement fusion targets.* Phys. Plasmas **7,** 1531 (2000)
4. O. Mannion, Private communication
5. C.K. Li and R. D. Petrasso, *Charged-Particle Stopping Powers in Inertial Confinement Fusion Plasmas,* Phys. Rev. **70,** 3059 (1993)
6. F. Weilacher et al., *Three-dimensional modeling of the neutron spectrum to infer plasma conditions in cryogenic inertial confinement fusion implosions,* Phys. Plasmas 25, 042704 (2018)
7. Lowell S. Brown, Dean L. Preston, and Robert L. Singleton Jr, *Charged Particle Motion in a Highly Ionized Plasma*. Phys. Plasmas 0501084 (2007).